Electronic Supplementary Information

Asymmetric Rhenium Tricarbonyl Complexes Show Superior Luminescence Properties in Live Cell Imaging

Lukasz J. Raszeja,[a)] Daniel Siegmund,[a)] Anna L. Cordes,[a)] Jörn Güldenhaupt,[b)] Klaus Gerwert,[b)] and Nils Metzler-Nolte[a)*]

a) Faculty of Chemistry and Biochemistry, Inorganic Chemistry I – Bioinorganic Chemistry, Ruhr-University Bochum, Universitätsstr. 150, 44801 Bochum, Germany; b) Faculty of Biology and Biotechnology, Chair of Biophysics, Ruhr-University Bochum, Universitätsstr. 150, 44801 Bochum, Germany. E-mail: nils.metzler-nolte@rub.de

Contents

1. Experimental: General Remarks

Commercial purchased reagents were used without any further purification. Solvents needed for synthesis were of analytical grade and for spectroscopic investigations of spectroscopical grade. Degassed acetonitrile was obtained by the freeze-pump-thaw procedure, applying for at least three cycles. All reported compounds were confirmed to be pure by NMR, HPLC, HRMS or elemental analysis. NMR spectra were recorded on a Bruker DRX 400 (400 MHz for ^{1}H, 101 MHz for ^{13}C) or on a Bruker DPX 200 (200 MHz for ^{1}H, 50 MHz for ^{13}C), where the deuterated solvent was used as internal standard. IR spectra were recorded on a Bruker Tensor 27, ESI Mass spectra on a Bruker Esquire 6000 and EI High Resolution Mass Spectra on a Fisons VG Autospec. Elemental analysis was performed on a Foss Heraeus Vario EL. UV-vis spectra were recorded on a JASCO V-670 spectrophotometer by using a 1 cm cuvette. Steady state emission spectra and luminescence quantum yields were acquired on a PTI Quantamaster QM4 spectrofluorimeter using 1.0 cm quartz cuvettes at 298 K. The excitation light source was a 75 W continuous xenon short arc lamp. Emission spectra were collected at 90° to the excitation beam using a PTI R928 photomultiplier tube as the detector. Luminescence quantum yields were determined by the comparative method[1] using Tris(2,2'-bipyridyl)ruthenium(II) chloride in aerated water ($\Phi = 0.028$[2]) as reference. Lifetime measurements were carried out by means of time correlating single photon counting and were performed with a setup from Picoquant (Berlin, Germany). The setup consisted of a pulsed laserdiode, emitting at 375 nm (LDH-P-C-470B, pulse width at FWHH < 70 ps) driven by the laser driver PDL 800-D at 125 kHz, a photomultiplier detector module (PMA 182-N-M) equipped with a 430 nm longpass cut-off filter and a time correlating device (Picoharp 300). The ratio between incoming photons and laser flashes was kept lower than 3% by adjusting the laser power. The photon events were stored in histogram bins of 512 ns time width and the integration time for each histogram was 30 min. Because of the more than thousand times longer decay time of the sample signal than of the system IRF (instrument response function), the data was analysed by simple multi exponential fitting without using IRF reconvolution fitting. All samples were measured at room temperature in a concentration of 100 μM.

2. Syntheses and Characterizing Data

The syntheses of the starting materials such as 6-(chloromethyl)phenanthridine and 4-aminomethyl benzoic acid methyl ester were described previously.[3]

4-[(bis(6-phenanthridinylmethyl)amino)methyl]benzoic acid methyl ester (bpm) **1**

A white suspension consisting of 6-(chloromethyl)phenanthridine hydrochloride (600 mg, 2.27 mmol), 4-(aminomethyl)benzoic acid methyl ester hydrochloride (206 mg, 1.02 mmol, 0.45 eq.) and K_2CO_3 (1.57 g, 11.35 mmol, 5 eq.) in 20 ml of acetonitrile was heated under reflux for 48 h. After cooling to room temperature the orange suspension was evaporated to dryness. The orange residue was diluted with 30 ml of a half-saturated $NaHCO_3$ solution and 30 ml of chloroform. After rigorous mixing the phases were separated. The organic solution was washed twice with 20 ml of a saturated $NaHCO_3$ solution and dried over $MgSO_4$. After evaporating the solvent, the red-brownish, oily residue was purified by column chromatography on silica, eluting with ethyl acetate/*n*-hexane (1:1) first, then with ethyl acetate. The 4-[(bis(6-phenanthridinylmethyl)amino)methyl]benzoic acid methyl ester was obtained as a yellowish, foamy solid in 94.1% (525 mg, 0.96 mmol) yield.

^{1}H NMR (400 MHz, $CDCl_3$) δ: 8.55 (d, *J* = 8.3 Hz, 2H), 8.50 (dd, *J* = 8.2 Hz, 1.0 Hz, 2H), 8.16 (dd, *J* = 8.1 Hz, 1.1 Hz, 2H), 8.01 (d, *J* = 8.2 Hz, 2H), 7.87 (d, *J* = 8.3 Hz, 2H), 7.74 (dt, *J* = 7.7 Hz, 1.1 Hz, 2H), 7.70 (dt, *J* = 7.5 Hz, 1.4 Hz, 2H), 7.62 (dt, *J* = 7.6 Hz, 1.4 Hz, 2H), 7.33 – 7.18 (m, 4H), 4.42 (s, 4H), 3.88 (2 s, 5H) ppm. ^{13}C NMR (101 MHz, $CDCl_3$) δ: 167.2, 158.6, 144.3, 143.7, 133.1, 130.6, 130.3, 130.0, 129.5, 129.2, 128.8, 128.0, 127.1, 126.8, 125.7, 124.4, 122.1, 122.1, 61.0, 59.5, 52.2 ppm. MS (ESI$^+$): m/z = 548.09 $[M+H]^+$, 570.08 $[M+Na]^+$. UV/vis (CH_3CN), λ_{max}, nm (ε, $M^{-1}cm^{-1}$): 332 (3143), 348 (2884). IR (ATR): ν_{max} (cm^{-1}) = 1717 ($COOCH_3$). $C_{31}H_{25}N_3O_2$ calculated C, 78.96; H, 5.34; N, 8.91; calculated for $C_{31}H_{25}N_3O_2$ * ½ $CH_3COOCH_2CH_3$ C, 79.16; H, 5.62; N, 7.10; found C, 79.17; H, 5.60; N, 7.02.

4-[((6-phenanthridinylmethyl)(2-picolyl)amino)methyl]benzoic acid methyl ester (pmpi) **2**

A white suspension consisting of 6-(chloromethyl)phenanthridine (178 mg, 0.78 mmol), 4-[((2-picolyl)amino)methyl]benzoic acid methyl ester (200 mg, 0.78 mmol) and K_2CO_3 (216 mg, 1.56 mmol) in 12 ml of acetonitrile was heated under reflux for 20 h. After cooling to room temperature the orange suspension was evaporated to dryness. The orange-red residue was diluted with 10 ml of a half-saturated $NaHCO_3$ solution and 10 ml of chloroform. After rigorous mixing the phases were separated. The aqueous phase was extracted once with 10 ml of chloroform. The combined organic phases were dried over $MgSO_4$ and the solvent was evaporated. The red-brownish, oily residue was purified by column chromatography on silica, eluting with ethyl acetate/*n*-hexane in gradient mode. 4-[((6-phenanthridinylmethyl)(2-picolyl)amino)methyl]benzoic acid methyl ester was obtained as a yellowish, highly viscous oil in 89.7% (315 mg, 0.70 mmol) yield.

^{1}H NMR (400 MHz, $CDCl_3$) δ: 8.31 (d, *J* = 8.3 Hz, 1H), 8.24 (dd, *J* = 8.1 Hz, 1.3 Hz, 1H), 8.20 (ddd, *J* = 4.9 Hz, 1.7 Hz, 0.8 Hz, 1H), 8.02 (d, *J* = 8.3 Hz, 1H), 7.85 (dd, *J* = 8.1 Hz, 1.2 Hz, 1H), 7.58 (d, *J* = 8.3 Hz, 2H), 7.54 (ddd, *J* = 8.2 Hz, 7.1 Hz, 1.2 Hz, 1H), 7.41 (ddd, *J* = 8.2 Hz, 7.1 Hz, 1.4 Hz, 1H), 7.37 - 7.30 (m, 4H), 7.15 (d, *J* = 8.2 Hz, 2H), 7.10 (d, *J* = 7.8 Hz, 1H), 4.17 (s, 2H), 3.72 (s, 2H), 3.63 (s, 2H), 3.56 (s, 3H) ppm. ^{13}C NMR (101 MHz, $CDCl_3$) δ: 166.3, 157.6, 148.2, 143.3, 142.5, 137.2, 136.3, 132.6, 130.5, 129.2, 129.1, 129.0, 128.8, 128.3, 127.0, 126.8, 126.7, 124.9, 123.8, 123.5, 122.0, 121.8, 121.7, 59.9, 59.3, 58.3, 51.4 ppm. MS (ESI$^+$): m/z = 448.08 $[M+H]^+$, 470.03 $[M+Na]^+$. $C_{29}H_{25}N_3O_2$ calculated C, 77.83; H, 5.63; N, 9.39; calculated for $C_{31}H_{25}N_3O_2$ * ¼ $CHCl_3$: C, 73.59; H, 5.33; N, 8.80; found C, 73.25; H, 5.15; N, 8.68.

4-[((6-phenanthridinylmethyl) (2-quinolinylmethyl)amino)methyl]benzoic acid methyl ester (qmpm) **3**

A white suspension consisting of 6-(chloromethyl)phenanthridine (132 mg, 0.58 mmol), 4-[((2-quinolinylmethyl)amino)methyl]benzoic acid methyl ester (179 mg, 0.58 mmol) and K_2CO_3 (160 mg, 1.16 mmol) in 10 ml of acetonitrile was heated under reflux for 24 h. After cooling to room temperature the orange suspension was evaporated to dryness. The orange-red residue was diluted with 10 ml of a half-saturated $NaHCO_3$ solution and 10 ml of chloroform. After rigorous mixing the phases were separated. The aqueous phase was extracted twice with 7 ml of chloroform. The combined organic phases were dried over $MgSO_4$ and the solvent was evaporated. The orange residue was purified by column chromatography on silica, eluting with ethyl acetate/*n*-hexane in gradient mode. 4-[((6-phenanthridinylmethyl)(2-quinolinylmethyl)amino)methyl]benzoic acid methyl ester was obtained as a yellowish, foamy solid in 91.4% (265 mg, 0.53 mmol) yield.

NMR (400 MHz, $CDCl_3$) δ: 8.55 (d, *J* = 8.3 Hz, 1H), 8.49 (dd, *J* = 8.2 Hz, 1.2 Hz, 1H), 8.33 (d, *J* = 7.8 Hz, 1H), 8.18 (d, *J* = 8.0 Hz, 1H), 8.08 (d, *J* = 8.5 Hz, 1H), 8.04 (d, *J* = 8.5 Hz, 1H), 7.92 (d, *J* = 8.5 Hz, 2H), 7.81 (td, *J* = 7.1 Hz, 1.2 Hz, 1H), 7.76 (dd, *J* = 8.2 Hz, 0.9 Hz, 1H), 7.70 (td, *J* = 7.0 Hz, 1.3 Hz, 1H), 7.69 (td, *J* = 7.0 Hz, 1.3 Hz, 1H), 7.63 (td, *J* = 6.9 Hz, 1.4 Hz, 1H), 7.58 (t, *J* = 7.7 Hz, 1H), 7.50 (td, *J* = 7.0 Hz, 1.1 Hz, 1H), 7.47 (d, *J* = 8.1 Hz, 1H), 7.46 (d, *J* = 8.5 Hz, 2H), 4.53 (s, 2H), 4.19 (s, 2H), 3.99 (s, 2H), 3.88 (s, 3H) ppm. ^{13}C NMR (101 MHz, $CDCl_3$) δ: 167.1 , 159.4, 158.1, 147.3, 144.0, 143.2, 136.8, 133.3, 130.9, 130.0, 129.9, 129.8, 129.7,

129.4, 129.0, 128.9, 127.7, 127.6, 127.5, 127.3, 127.2, 126.7, 125.5, 124.4, 122.3, 122.1, 121.7, 61.2, 60.1, 59.2, 52.2. MS (ESI^+): m/z = 498.13 $[M+H]^+$, 520.07 $[M+Na]^+$. $C_{33}H_{27}N_3O_2$ calculated C, 79.66; H, 5.47; N, 8.44; calculated for $C_{33}H_{27}N_3O_2$ * ¼ $CH_3COOCH_2CH_3$ C, 78.59; H, 5.63; N, 8.09; found C, 78.78; H, 5.03; N, 8.34.

General procedure for the synthesis of *fac*-[$Re(CO)_3$] complexes **4-6**

$[Re(CO)_3(H_2O)_3]Br$ (40.4 mg, 100 µmol) was suspended together with the ligand (**1**-**3**) in 4 ml of methanol. Then the mixture was stirred in a CEM discovery microwave reactor for 10 min at 110 °C. The resulting dark red solution was concentrated to about a half and filtered through a PTFE filter (22 µm). The solution was finally layered with cold diethyl ether. Crystallization occurred over night at room temperature and yielded light beige to colourless crystals. These were filtered and dried in air.

fac-[$Re(CO)_3$(bpm)]bromide **4**

Yield: 74.6% (67.0 mg, 74.6 µmol)

^1H NMR (400 MHz, DMSO) δ: 8.94 (2d, *J* = 8.9 Hz, 4H), 8.47 - 8.41 (m, 2H), 8.23 (t, *J* = 8.6 Hz, 2H), 8.21 (d, *J* = 3.7 Hz, 2H), 8.17 (d, *J* = 8.5 Hz, 2H), 8.11 (t, *J* = 7.7 Hz, 2H), 7.94 - 7.78 (m, 6H), 5.99 (d, *J* = 18.5 Hz, 2H), 5.69 (d, *J* = 18.6 Hz, 2H), 5.33 (s, 2H), 3.94 (s, 3H) ppm. ^{13}C NMR (101 MHz, DMSO) δ: 196.2, 194.3, 167.6, 166.0, 141.2, 137.3, 134.5, 133.3, 132.4, 130.5, 130.4, 129.6, 129.4, 128.9, 127.9, 124.8, 124.2, 123.99, 122.98, 122.95, 68.4, 66.8, 52.3 ppm. MS (ESI^+): m/z = 817.91 $[M]^+$. IR (ATR): ν_{max} (cm^{-1}) = 2027, 1920 (*fac*-$Re(CO)_3$), 1700 ($COOCH_3$). UV/vis (CH_3CN), λ_{max}, nm (ε, $M^{-1}cm^{-1}$): 310 (13400), 350 (10600), 360 (9000).

fac-[$Re(CO)_3$(pmpi)]bromide **5**

Yield: 80.2% (64.0 mg, 80.2 µmol)

^1H NMR (400 MHz, DMSO) δ: 9.06 (d, *J* = 5.2 Hz, 1H), 8.95 (d, *J* = 9.5 Hz, 1H), 8.93 (d, *J* = 9.0 Hz, 1H), 8.59 (d, *J* = 7.8 Hz, 1H), 8.24 (d, *J* = 8.3 Hz, 1H), 8.17 (d, *J* = 8.3 Hz, 2H), 8.14 (t, *J* = 7.9 Hz, 1H), 8.11 (d, *J* = 8.4 Hz, 2H), 8.03 - 7.99 (m, 1H), 7.99 - 7.95 (m, 1H), 7.92 - 7.89 (m, 1H), 7.89 - 7.86 (m, 1H), 7.59 (d, *J* = 7.9 Hz, 1H), 7.47 (td, *J* = 6.2 Hz, 0.9 Hz, 1H), 5.89 (d, *J* = 17.6 Hz, 1H), 5.63 (d, *J* = 17.6 Hz, 1H), 5.15 (s, 2H), 5.05 (d, *J* = 17.3 Hz, 1H), 4.63 (d, *J* = 17.3 Hz, 1H), 3.93 (s, 3H) ppm. ^{13}C NMR (101 MHz, DMSO) δ: 195.4, 195.1, 194.6, 166.5, 166.0, 161.4, 152.5, 141.3, 140.5, 137.1, 134.6, 133.1, 132.5, 130.4, 130.4, 129.5, 129.4, 129.1, 128.9, 128.0, 125.7, 124.7, 124.0, 123.7, 123.1, 123.0, 69.1, 66.6, 65.3, 52.3 ppm. MS (ESI^+): m/z = 717.93 $[M]^+$. IR (ATR): ν_{max} (cm^{-1}) = 2028, 1925, 1892 (*fac*-$Re(CO)_3$), 1720 ($COOCH_3$). UV/vis (CH_3CN), λ_{max}, nm (ε, $M^{-1}cm^{-1}$): 310 (9600), 350 (7300), 360 (6000).

fac-[$Re(CO)_3$(pmqm)]bromide **6**

Yield: 76.7% (65.0 mg, 76.7 µmol)

^1H NMR (400 MHz, DMSO) δ: 8.93 (d, *J* = 8.2 Hz, 1H), 8.93 - 8.90 (m, 1H), 8.67 (d, *J* = 8.4 Hz, 1H), 8.43 (d, *J* = 8.7 Hz, 1H), 8.41 - 8.38 (m, 1H), 8.18 (d, *J* = 7.8 Hz, 1H), 8.17 (d, *J* = 7.0 Hz, 1H), 8.15 (d, *J* = 8.4 Hz, 2H), 8.13 (d, *J* = 8.3 Hz, 2H), 8.11 (td, *J* = 7.2 Hz, 0.8 Hz, 1H), 8.00 (td, *J* = 7.1 Hz, 1.5 Hz, 1H), 7.87 (td, *J* = 7.4 Hz, 0.7 Hz, 1H), 7.85 - 7.81 (m, 2H), 7.77 (td, *J* = 7.2 Hz, 0.7 Hz, 1H), 7.67 (d, *J* = 8.5 Hz, 1H), 5.92 (d, *J* = 18.3 Hz, 1H), 5.54 (d, *J* = 18.4 Hz, 1H), 5.43 (d, *J* = 18.1 Hz, 1H), 5.25 (s, 2H), 5.05 (d, *J* = 18.1 Hz, 1H), 3.93 (s, 3H) ppm. ^{13}C NMR (101 MHz, DMSO) δ: 196.2, 194.4, 194.1, 167.3, 166.0, 165.8, 146.0, 141.3, 141.2, 137.2, 134.6, 133.3, 133.0, 132.4, 130.5, 130.3, 129.9, 129.6, 129.5, 128.9, 128.8, 128.1, 127.9, 127.5, 124.7, 124.1, 123.1, 123.0, 120.4, 68.4, 67.9, 66.3, 52.4 ppm. MS (ESI^+): m/z = 767.92 $[M]^+$. IR (ATR): ν_{max} (cm^{-1}) = 2026, 1904 (*fac*-$Re(CO)_3$), 1722 ($COOCH_3$). UV/vis (CH_3CN), λ_{max}, nm (ε, $M^{-1}cm^{-1}$): 310 (13100), 320 (13500), 350 (8200), 360 (6600).

3. Crystallographic Data

Complexes **4** and **6**:

Crystal of **4** or **6** was mounted on a glass capillary in perflourinated oil and measured in a cold gas flow. The intensities were measured with on a Rigaku Mercury 375 R/M CCD (XtaLAB mini); ($Mo_{K\alpha}$ radiation, λ=0.7170 Å, ω scan). The structure was solved by direct methods (SHELXS97), and refined against F^2 with all measured reflections (SHELXL97). All non-hydrogen atoms were refined anisotropically and the hydrogen atoms were included in calculated positions. Crystallographic data (excluding structure factors) for the structures reported in this paper have been deposited with the Cambridge Crystallographic Data Centre as supplementary publication no. CCDC- 853881 (complex **4**) and CCDC-853882 (complex **6**). Copies of the data can be obtained free of charge on application to CCDC, 12 Union Road, Cambridge CB2 1EZ, UK [Fax: int. code + 44(1223)336-033; E-mail: deposit@ccdc.cam.ac.uk].

Complex **5**.

The X-ray diffraction intensities were collected on an Oxford Xcalibur2 diffractometer with a Sapphire2 CCD. A Crystal of **5** was coated with a perfluoropolyether, picked up with a glass fibre, and immediately mounted in the

cooled nitrogen stream of the diffractometer. The structure was solved by direct methods (SHELXS97), and refined against F^2 with all measured reflections (SHELXL97). All non-hydrogen atoms were refined anisotropically and the hydrogen atoms were included in calculated positions. Crystallographic data (excluding structure factors) for the structures reported in this paper have been deposited with the Cambridge Crystallographic Data Centre as supplementary publication no. CCDC-853883. Copies of the data can be obtained free of charge on application to CCDC, 12 Union Road, Cambridge CB2 1EZ, UK [Fax: int. code + 44(1223)336-033; E-mail: deposit@ccdc.cam.ac.uk].

Complex **4**:

$C_{41}H_{32}BrN_3O_6Re$, M = 928.81, space group *C2/c*, *a* = 19.79(4), *b* = 14.87(3), *c* = 25.04(4) Å, α = 90 °, β = 100.33(3) °, γ = 90 °, *V* = 7249(24) Å^3.

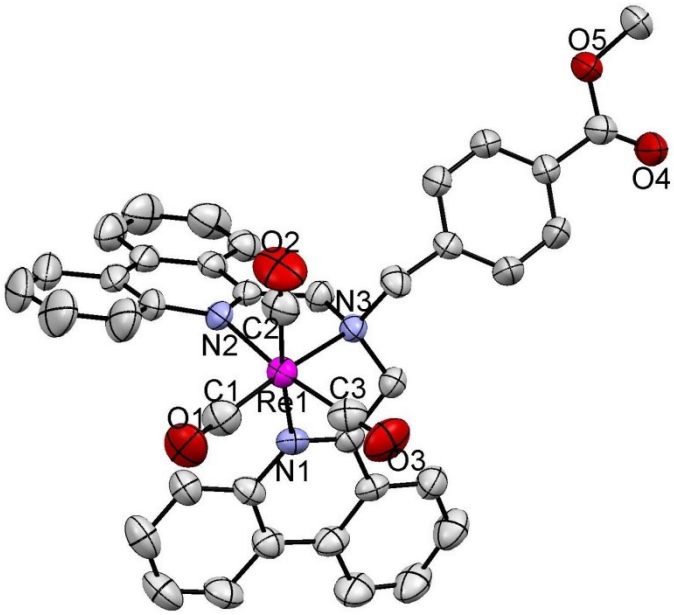

ORTEP plot of complex **4** (50% probability, hydrogen atoms, cocrystallized CH_3OH and bromide counterion omitted for clarity).

Complex **5**:

$C_{34}H_{31}BrN_3O_7Re$, M = 859.73, space group *P21/n*, *a* = 14.2253(4), *b* = 13.4844(3), *c* = 19.7773(4) Å, α = 90 °, β = 109.927(3) °, γ = 90 °, *V* = 3566.54(16) Å^3.

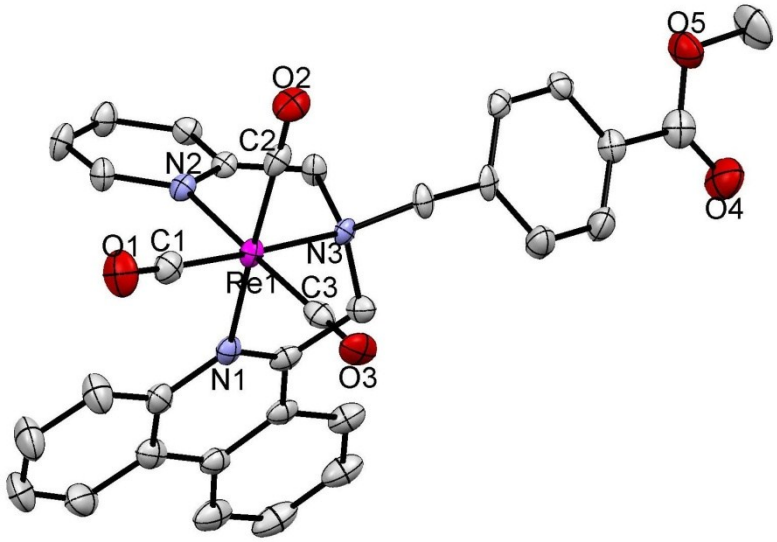

ORTEP plot of complex **5** (50% probability, hydrogen atoms, cocrystallized CH_3OH and bromide counterion omitted for clarity).

Complex **6**:
$C_{38}H_{33}BrN_3O_7Re$, M = 909.78, space group *P21/n*, *a* = 13.791(2), *b* = 13.5301(15), *c* = 20.451(4) Å, α = 90 °, β = 108.728(6) °, γ = 90 °, *V* = 3614.0(10) Å^3.

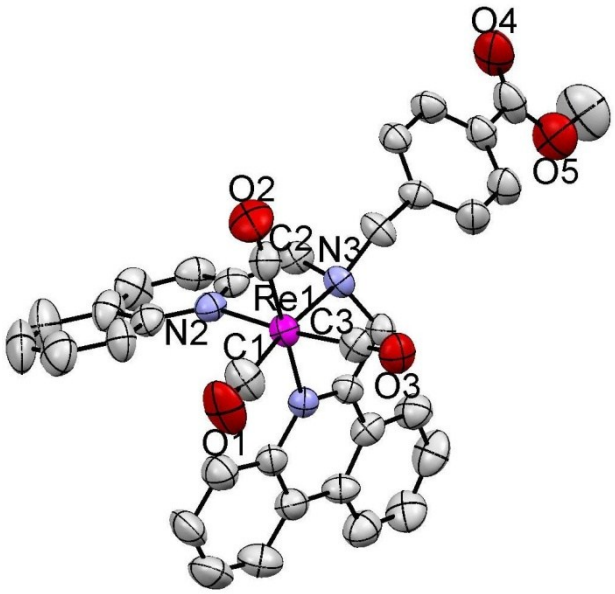

ORTEP plot of complex **6** (50% probability, hydrogen atoms, cocrystallized CH_3OH and bromide counterion omitted for clarity).

4. Cell Culture and Imaging

Dulbecco's Modified Eagle's Medium (DMEM) supplemented with 10% fetal bovine serum, penicillin and streptomycine was used as growth medium. Cells were detached from the wells using trypsin and EDTA, harvested by centrifugation (300 g, 3 min) and resuspended again in cell culture medium. The cells were seeded on 8 well ibidi µ–Slide plates in a concentration of 30.000 cells per well (120.000 cells per ml) and incubated for 24 h. The cells were washed with PBS (pH 7.4) prior to incubation with the rhenium complexes. After incubation the cells were washed with PBS (pH 7.4) and covered with medium for the microscopic examinations. The imaging experiments were made on an OLYMPUS IX81 fluorescence microscope by using a filter system consisting of an excitation filter for excitation between 326 nm and 375 nm, a 455 nm dichroic mirror and a long pass emission filter for wavelengths higher than 510 nm for detection. The used platform was cell^M 3.2 (Build 1700). Colocalization experiments were carried out using commercially available organelle stains and rhenium complexes in 5 to 10 µM concentration and an incubation time of 3-4 h. Thereby, the procedures for organelle staining were taken from the supplied manuals provided by the manufacturer. Organelle stains: Endoplasmic reticulum: ER-ID™ Red Assay Kit (Enzo® Life Sciences), Golgi apparatus: Golgi-ID™ Green Assay Kit (Enzo® Life Sciences), mitochondria: MitoTracker® Deep Red FM (Invitrogen™/Molecular Probes), DNA: DRAQ5™ (ThermoFischer Scientific).

4a Colocalization studies for complex 4 on IMIM-PC2 cells using different commercial stains

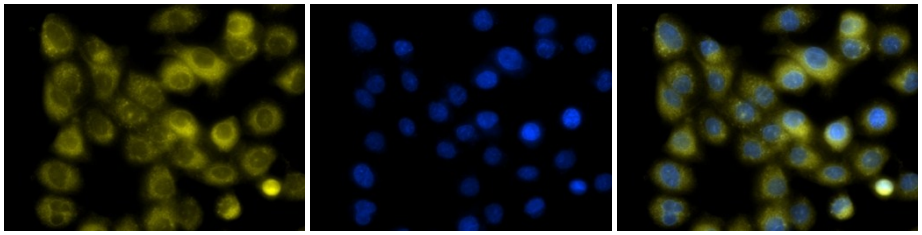

Figure 1: IMIM-PC2 cells (200x magnification) incubated with **4** (10 µM, 3 h, 37°C, 10% CO_2) and DRAQ5™. Left: luminescence of complex **4** (artificial colour), middle: commercial stain DRAQ5™, right: merged.

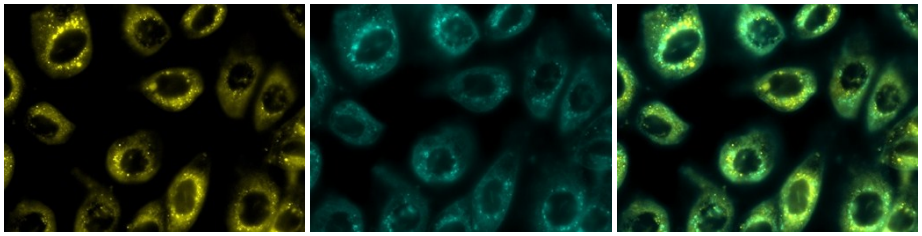

Figure 2: IMIM-PC2 cells (600x magnification) incubated with **4** (5 µM, 4 h, 37°C, 10% CO_2) and GOLGI-ID™ green. Left: luminescence of complex **4** (artificial colour), middle: commercial stain GOLGI-ID™ green, right: merged.

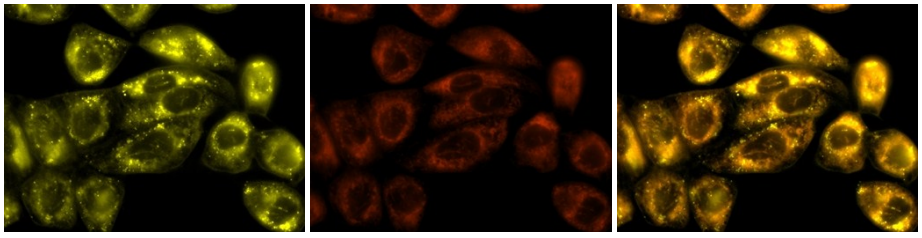

Figure 3: IMIM-PC2 cells (600x magnification) incubated with **4** (5 µM, 4 h, 37°C, 10% CO_2) and MitoTracker® deep red. Left: luminescence of complex **4** (artificial colour), middle: commercial stain MitoTracker® deep red, right: merged.

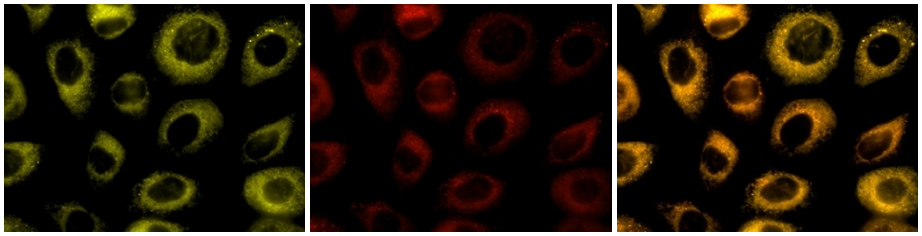

Figure 4: IMIM-PC2 cells (600x magnification) incubated with **4** (5 µM, 3 h, 37°C, 10% CO_2) and ER-ID™ red. Left: luminescence of complex **4** (artificial colour), middle: commercial stain ER-ID™ red, right: merged.

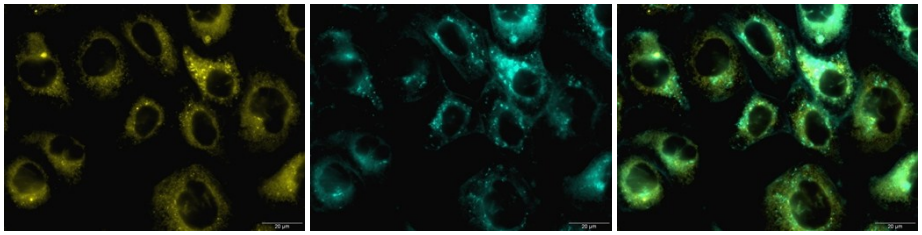

Figure 5: IMIM-PC2 cells (600x magnification) incubated with **6** (5 µM, 5 h, 37°C, 10% CO_2) and GOLGI-ID™. Left: luminescence of complex **6** (artificial colour), middle: commercial stain GOLGI-ID™ green, right: merged.

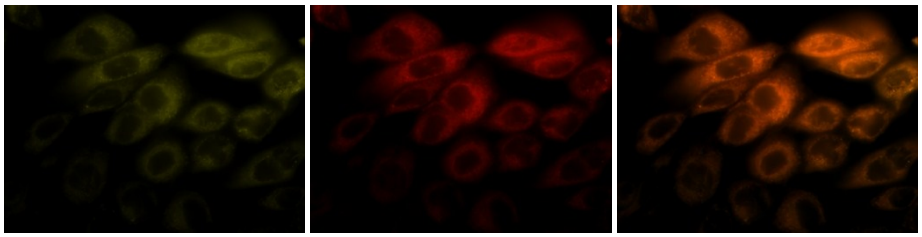

Figure 6: IMIM-PC2 cells (600x magnification) incubated with **6** (5 µM, 90 min, 37°C, 10% CO_2) and ER-ID™ red. Left: luminescence of complex **6** (artificial colour), middle: commercial stain ER-ID™ red, right: merged.

4b Colocalization studies of complex 4 on different cell lines

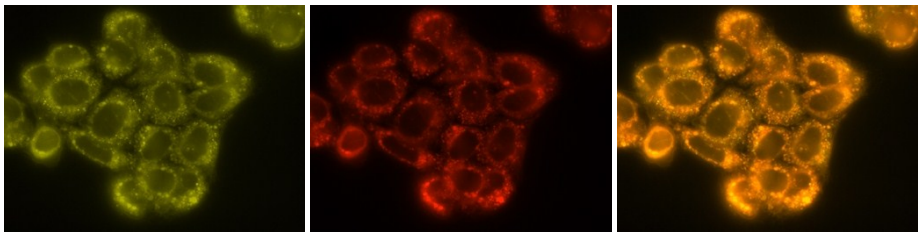

Figure 7: Hep G2 cells (600x magnification) incubated with **4** (5 µM, 5 h, 37°C, 10% CO_2) and ER-ID™ red. Left: luminescence of complex **4** (artificial colour), middle: commercial stain ER-ID™ red, right: merged.

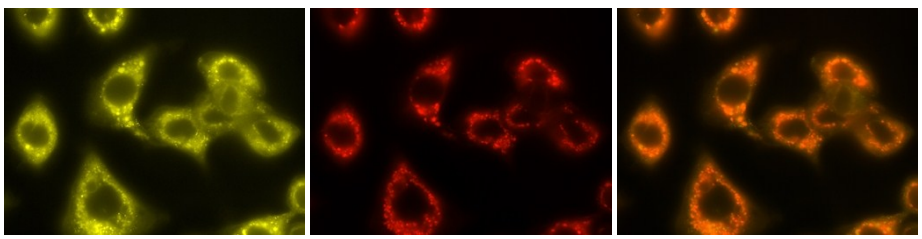

Figure 8: MCF-7 cells (600x magnification) incubated with **4** (5 µM, 5 h, 37°C, 10% CO_2) and ER-ID™ red. Left: luminescence of complex **4** (artificial colour), middle: commercial stain ER-ID™ red, right: merged.

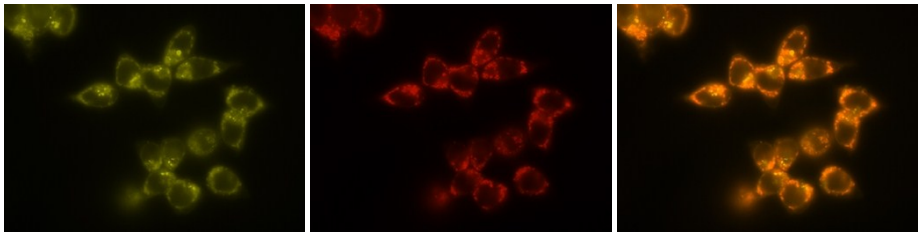

Figure 9: HT29 cells (400x magnification) incubated with **4** (5 µM, 5 h, 37°C, 10% CO_2) and ER-ID™ red. Left: luminescence of complex **4** (artificial colour), middle: commercial stain ER-ID™ red, right: merged.

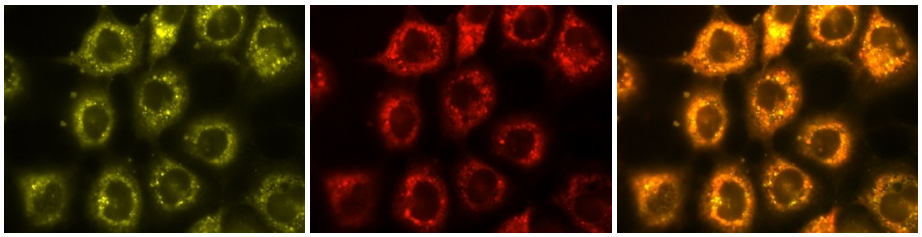

Figure 10: PT45 cells (600x magnification) incubated with **4** (5 µM, 5 h, 37°C, 10% CO_2) and ER-ID™ red. Left: luminescence of complex **4** (artificial colour), middle: commercial stain ER-ID™ red, right: merged.

4c Photostability

To demonstrate the photostability of our compounds we compared complex **6** to the commercial stains ER-ID™ and Golgi-ID™ under microscopy imaging conditions. For this, MCF-7 cells were seeded into ibidi µ–Slide plates (50 000 cells/well) and incubated for 24 h. Subsequently the cells were washed with PBS and fixed with freshly prepared 3,7% formaldehyde in PBS (10 min, 37°C). The fixed cells were carefully rinsed with PBS (3x) and stained with the commercial dyes as described in the corresponding manuals provided by the manufacturers. In case of complex **6** the MCF-7 cells were treated with the compound (5 µM, 4 h) prior to fixation to ensure correct localization in the targeted organelle. The prepared samples were observed under constant illumination with the OLYMPUS IX81 fluorescence microscope described above. Pictures were taken every 10 seconds using constant settings.

Complex **6:**

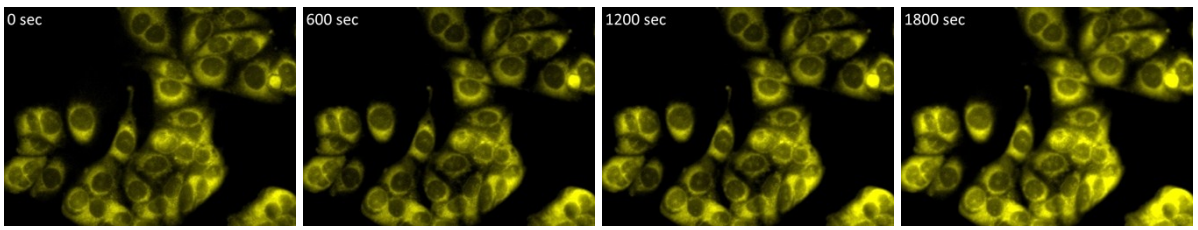

Figure 11: Luminescence of complex **6** on fixed MCF-7 cells (200x magnification).

ER-ID™:

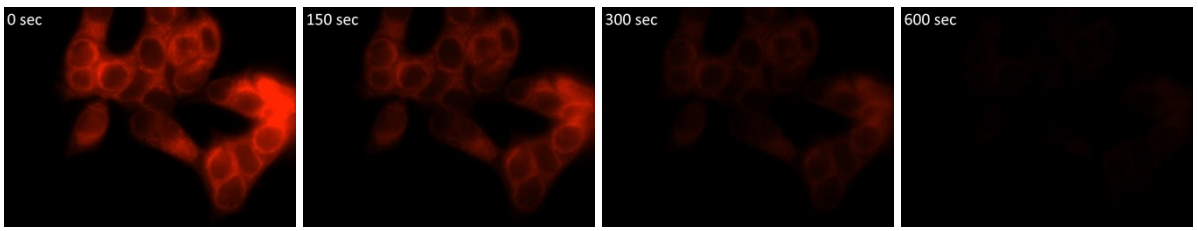

Figure 12: Luminescence of ER-ID™ on fixed MCF-7 cells (400x magnification).

Golgi-ID™:

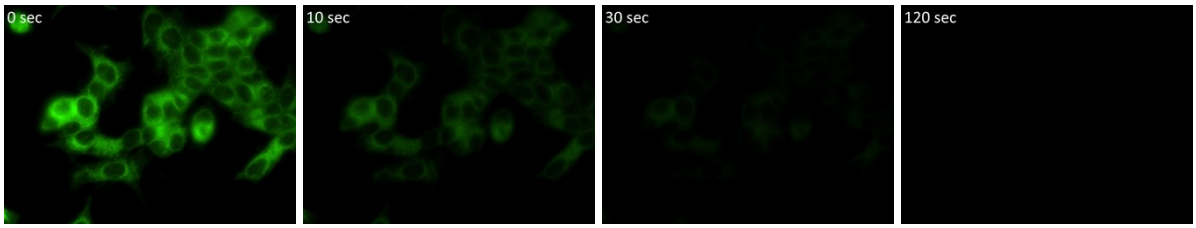

Figure 13: Luminescence of Golgi-ID™ on fixed MCF-7 cells (200x magnification).

5. Computational Details

5a General remarks

Quantum chemical calculations were performed using the GAUSSIAN09 program package (Rev. A.02).[4]
Ground state (S_0) geometries were optimized (without any symmetry restrictions) at the DFT level using the hybrid functional PBE0 (PBE1PBE in Gaussian) featuring 25% exchange and 75% correlation.[5] The double-ζ LANL2DZ basis set and an effective core potential by Hay and Wadt was used to describe the rhenium atoms.[6] For all other atoms (C H N O) the 6-31G* basis set was used. In previous studies by other groups, this level of theory has been found to provide a reliable model for *fac*-Re(I)$(CO)_3$ complexes.[7] Frequency calculations on the basis of the optimized geometries were performed to ensure the absence of imaginary frequencies, thus the obtained structures represent local minima on the energy surface. The vertical excitation energies were calculated by TD-DFT on the basis of the optimized ground state structures. The solvent effect of acetonitrile was included by applying the conductor-like polarized continuum model (CPCM). The GaussSum program package was used to calculate the depicted electron density difference maps.[8]

5b Comparison of bond lengths and angles

Table 1: Selected bond lengths and angles of complexes **4 - 6** determined by crystal structure (Exp.) and DFT-optimization (S_0, PBE0/LANL2DZ).

Bond lengths [Å] and Angles [°]

	Complex 4		**Complex 5**		**Complex 6**	
	Exp.	**S_0**	**Exp.**	**S_0**	**Exp.**	**S_0**
Re1-C1	1.909	1.915	1.918	1.912	1.924	1.914
Re1-C2	1.913	1.912	1.918	1.912	1.907	1.912
Re1-C3	1.925	1.912	1.925	1.922	1.916	1.911
Re1-N1	2.241	2.238	2.263	2.242	2.239	2.244
Re1-N2	2.223	2.241	2.167	2.184	2.230	2.247
Re1-N3	2.230	2.227	2.224	2.244	2.230	2.231
O4-C(O5)	1.200	1.215	1.212	1.215	1.211	1.215
O5-C(O4)	1.337	1.335	1.338	1.336	1.325	1.335
C1-Re1-N3	173.6	170.6	177.5	171.7	173.5	170.2
C2-Re1-N1	171.3	171.6	174.2	172.7	172.1	170.7
C3-Re1-N2	172.9	172.4	170.3	170.1	171.2	172.6

5c Calculated absorption properties

Table 2: Calculated absorptions of the complexes (TDDFT/PBE0 in acetonitrile (CPCM)) along with corresponding assignment. Only the most intense calculated contributions in each region were assigned to the relevant parts of the absorption spectra.

Complex	State	Contribution	Oscillator strenght	E(eV)	λ_{calc} [nm]	Major character	λ_{exp}[nm]
4	$S_0 \rightarrow S_1$	H → L (92%)	0.094	3.55	349	^{1}MLCT	350
	$S_0 \rightarrow S_4$	H - 3 → L (36%)	0.069	3.85	322	^{1}MLCT	
		H → L+1 (35%)				^{1}MLCT	
		H - 4 → L (14%)				^{1}MLCT/^{1}ILCT	
	$S_0 \rightarrow S_6$	H - 5 → L (44%)	0.0415	3.97	312	^{1}MLCT/^{1}ILCT	310
		H - 4 → L (43%)				^{1}MLCT/^{1}ILCT	
		H → L+1 (6%)				^{1}MLCT	
	$S_0 \rightarrow S_{32}$	H - 3→ L+4 (29%)	0.2972	4.99	248	^{1}MLCT/^{1}ILCT	250
		H - 1→ L+3 (23%)				^{1}IL/^{1}ILCT	
		H - 1→ L+4 (13%)				^{1}ILCT	
5	$S_0 \rightarrow S_1$	H - 1 → L (62%)	0.1039	3.68	338	^{1}IL/^{1}ILCT	350
		H → L (31%)				^{1}MLCT	
	$S_0 \rightarrow S_2$	H → L (62%)	0.1575	3.77	329	^{1}MLCT	325
		H - 1→ L (29%)				^{1}IL/^{1}ILCT	
	$S_0 \rightarrow S_4$	H - 2→ L (83%)	0.0162	3.91	317	^{1}MLCT/^{1}ILCT	310
		H - 3→ L (10%)				^{1}MLCT	
	$S_0 \rightarrow S_{22}$	H - 1 → L+3 (31%)	0.1701	4.99	249	^{1}IL/^{1}ILCT	250
		H - 7→ L (13%)				^{1}IL/^{1}ILCT	
		H - 3 → L+6 (9%)				^{1}MLCT	
		H - 9 → L (8%)				^{1}IL/^{1}ILCT	
		H - 2 → L+3 (8%)				^{1}ILCT/^{1}MLCT	
6	$S_0 \rightarrow S_1$	H → L (92%)	0.1305	3.57	347	^{1}MLCT	350
		H - 1 → L (2%)				^{1}ILCT	
	$S_0 \rightarrow S_2$	H - 1→ L (81%)	0.0666	3.75	331	^{1}ILCT	
		H - 1 → L+1 (6%)				^{1}IL/^{1}ILCT	
	$S_0 \rightarrow S_3$	H → L+1 (56%)	0.0495	3.86	321	^{1}MLCT	310
		H - 2 → L (32%)				^{1}ILCT	
		H - 3 → L (7%)				^{1}MLCT/^{1}ILCT	
	$S_0 \rightarrow S_{25}$	H - 1→ L+2 (56%)	0.0411	4.93	252	^{1}ILCT	250
		H - 1→ L+3 (21%)				^{1}ILCT	
		H - 2 → L+3 (7%)				^{1}IL/^{1}ILCT	
		H - 10 → L (6%)				^{1}ILCT	

5d Frontier molecular orbitals and electron density difference maps for absorption.

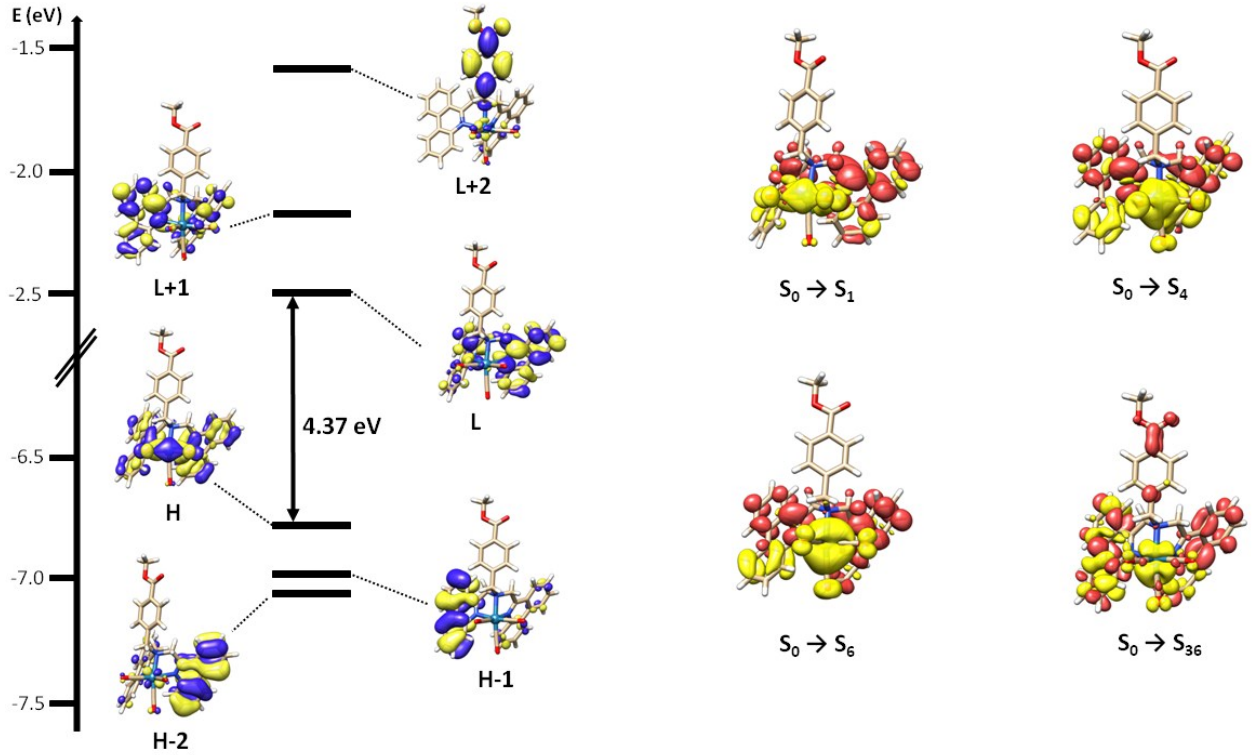

Figure 14: left: Partial molecular orbital diagram for complex **4**. right: Electron density difference plots for selected vertical transitions representative for several parts of the spectrum, computed at the TD-DFT (PBE0/LANL2DZ-CPCM) level of theory. Yellow and red indicate areas with decreasing and increasing electron density respectively. The calculated transitions show mixed MLCT/ILCT-character.

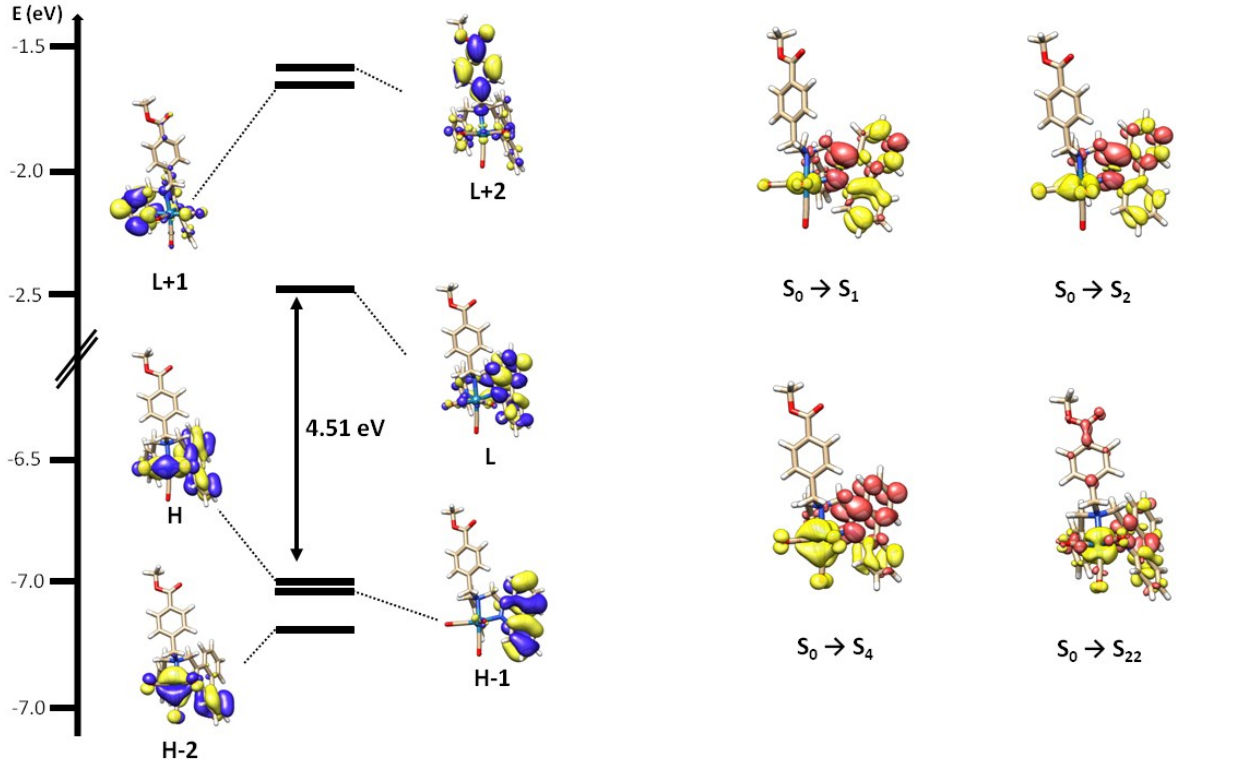

Figure 15: left: Partial molecular orbital diagram for complex **5**. right: Electron density difference plots for selected vertical transitions representative for several parts of the spectrum, computed at the TD-DFT (PBE0/LANL2DZ-CPCM) level of theory. Yellow and red indicate areas with decreasing and increasing electron density respectively. The calculated transitions show mixed MLCT/ILCT-character.

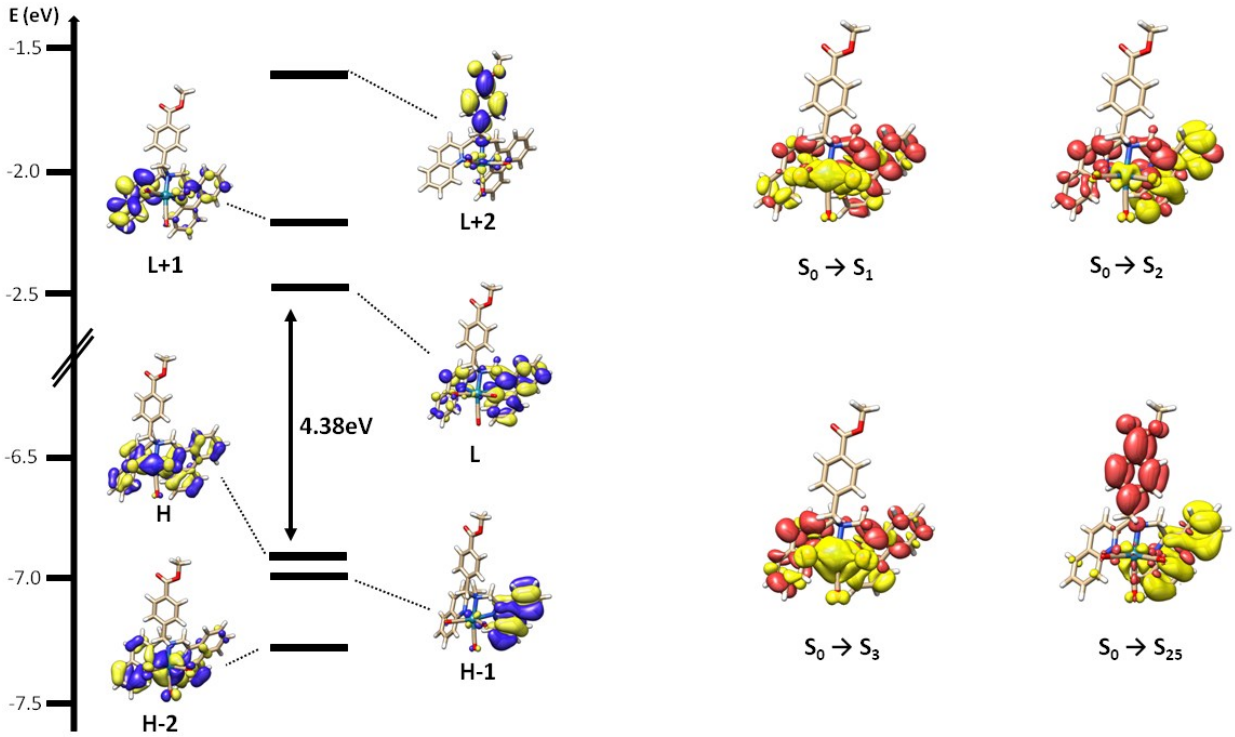

Figure 16: left: Partial molecular orbital diagram for complex **6**. right: Electron density difference plots for selected vertical transitions representative for several parts of the spectrum, computed at the TD-DFT (PBE0/LANL2DZ-CPCM) level of theory. Yellow and red indicate areas with decreasing and increasing electron density respectively. The calculated transitions show mixed MLCT/ILCT-character. In the higher energy part of the spectrum, ILCT transitions become dominant.

1 Crosby, G. A.; Demas, J. N. *J. Phys. Chem.,* 1971, **75**, 991.

2 Nakamaru, K. *Bull. Chem. Soc. Jpn.,* 1982, **55**, 2697.

3 Raszeja, L.; Maghnouj, A.; Hahn, S.; Metzler-Nolte, N. *ChemBioChem,* 2011, **12**, 371.

4 Gaussian 09, Revision A.02, Frisch, M. J.; Trucks, G. W.; Schlegel, H. B.; Scuseria, G. E.; Robb, M. A.; Cheeseman, J. R.; Scalmani, G.; Barone, V.; Mennucci, B.; Petersson, G. A.; Nakatsuji, H.; Caricato, M.; Li, X.; Hratchian, H. P.; Izmaylov, A. F.; Bloino, J.; Zheng, G.; Sonnenberg, J. L.; Hada, M.; Ehara, M.; Toyota, K.; Fukuda, R.; Hasegawa, J.; Ishida, M.; Nakajima, T.; Honda, Y.; Kitao, O.; Nakai, H.; Vreven, T.; Montgomery, J. A., Jr.; Peralta, J. E.; Ogliaro, F.; Bearpark, M.; Heyd, J. J.; Brothers, E.; Kudin, K. N.; Staroverov, V. N.; Kobayashi, R.; Normand, J.; Raghavachari, K.; Rendell, A.; Burant, J. C.; Iyengar, S. S.; Tomasi, J.; Cossi, M.; Rega, N.; Millam, J. M.; Klene, M.; Knox, J. E.; Cross, J. B.; Bakken, V.; Adamo, C.; Jaramillo, J.; Gomperts, R.; Stratmann, R. E.; Yazyev, O.; Austin, A. J.; Cammi, R.; Pomelli, C.; Ochterski, J. W.; Martin, R. L.; Morokuma, K.; Zakrzewski, V. G.; Voth, G. A.; Salvador, P.; Dannenberg, J. J.; Dapprich, S.; Daniels, A. D.; Farkas, Ö.; Foresman, J. B.; Ortiz, J. V.; Cioslowski, J.; Fox, D. J. Gaussian, Inc., Wallingford CT, 2009.

5 Adamo, C.; Barone, V. *J. Chem. Phys.*, 1999, **110,** 6158.

6 Hay, P. J.; Wadt, W. R. *J. Chem. Phys.* 1985, **82**, 299.

7. Velmurugan, G.; Ramamoorthi, B. K.; Venuvanalingam, P. *Phys. Chem. Chem. Phys*. 2014, **16**, 21157.

8. O'Boyle, N. M.; Tenderholt, A. L.; Langner, K. M. *J. Comp. Chem*. 2008, **29**, 839.